M. BENEDINI (*) - B. SIRANGELO (**) - S. TROISI (**) (***)
M. VURRO (***)

MATHEMATICAL MODEL OF A COASTAL AQUIFER SUBJECT TO SEAWATER INTRUSION: THE NARDÒ AQUIFER (ITALY) AS AN EXAMPLE

SUMMARY

Among groundwater management problems, one of the most higly studied is the exploitation of the freshwater « lens » that sometimes floats on top of the seawater in a coastal aquifer. General solutions, some relating to the entire aquifer, others to only parts of it, have been put forward utilizing a series of grids that represent the real situation with a various level of approximation.

In line with efforts to reproduce the complexities of a coastal aquifer, which is usually vertically and horizontally heterogeneous, the so-called Pinder's method, which takes both freshwater and saline water flows into consideration, deserves particular mention.

1. INTRODUCTION

There is an increasing tendency in groundwater studies towards a methodology for the optimal utilization of groundwater resources; i.e. an effort is made to pinpoint operational criteria (also based on « non physical » aspects such as economic, social and normative factors) allowing a choice to be made between the various possible ways of utilizing water drawn from an aquifer.

There are, however, a number of specific difficulties involved in these groundwater methodologies, which are mainly due to the fact that the physical characteristics of the filtering system (permeability, porosity, storage coef-

(*) Consiglio Nazionale delle Ricerche, Istituto di Ricerca Sulle Acque, Roma.
(**) Dipartimento Difesa del Suolo, Facoltà di Ingegneria, Università della Calabria.
(***) Consiglio Nazionale delle Ricerche, Istituto di Ricerca Sulle Acque, Laboratorio Sperimentale di Bari.

ficient, coefficient of dispersion, etc.) cannot be modified by man and affect the hydrodynamic aspects of the groundwater (regulation capacity, resistance to pollutant dispersion, propagation of hydraulic load variations) in a very complex and decisive manner inside the aquifer mass.

It is clear from the aforegoing that several interconnected models need to be prepared to describe the flow dynamics behaviour of an aquifer. The repre-

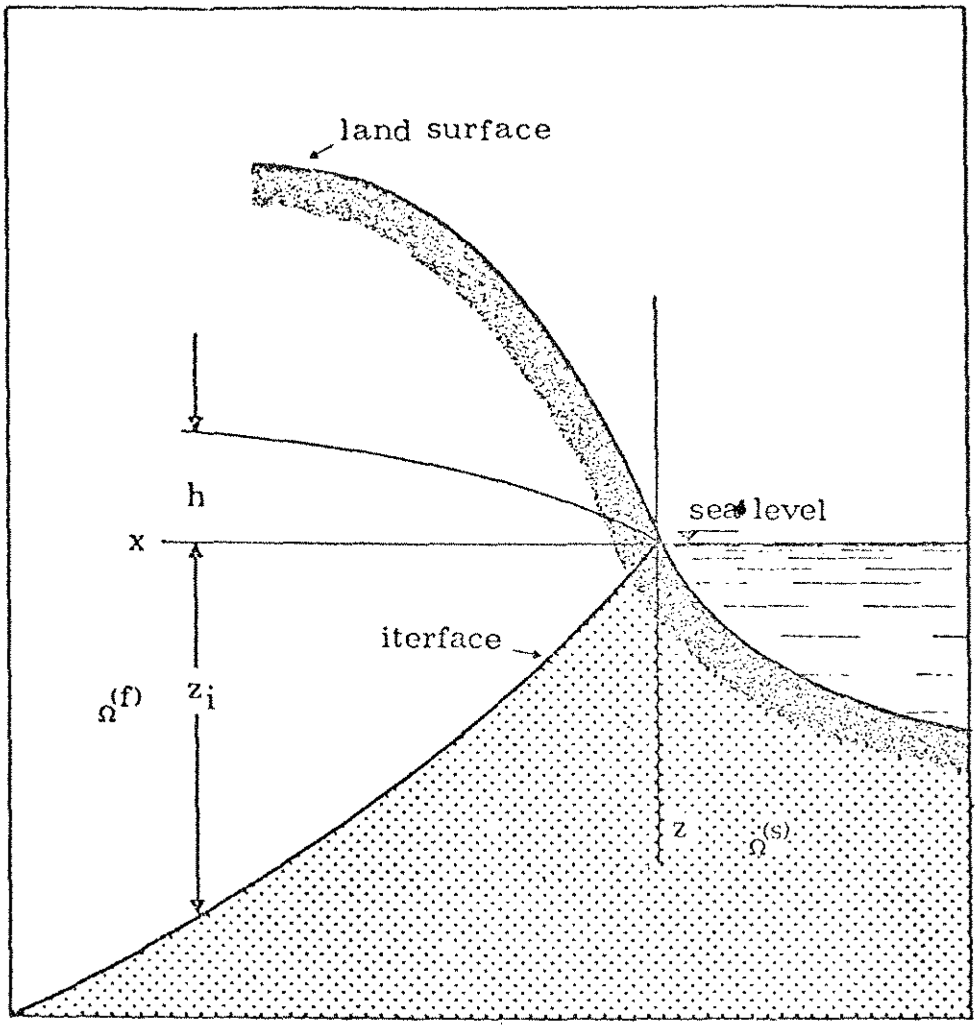

$$z_i = \frac{\varrho^{(f)}}{\varrho^{(s)} - \varrho^{(f)}} \cdot h$$

$\varrho^{(f)}, \varrho^{(s)}$: Freshwater and salt water density.

Fig. 1 - Ghyben-Herzberg's scheme and hydrostatic relation.

sentation thus obtained will be the most suitable for investigating the objectives set out above.

Among the problems of this kind being investigated by the Italia Water Research Institute, one of particular interest is that concerning the coastal aquifers and the utilization of the freshwater «lens» floating on top of the seawater. The aim of the present communication is to report on the application of an advanced methodology to an actual aquifer on the Salento peninsula [4].

2. APPROACH TO THE PROBLEM OF SEAWATER INTRUSION

A coastal aquifer, characterized by having at least one side of its perimeter in direct contact with the sea, besides being exposed to possible urban, industrial or agricultural pollution coming from the mainland, is highly subject

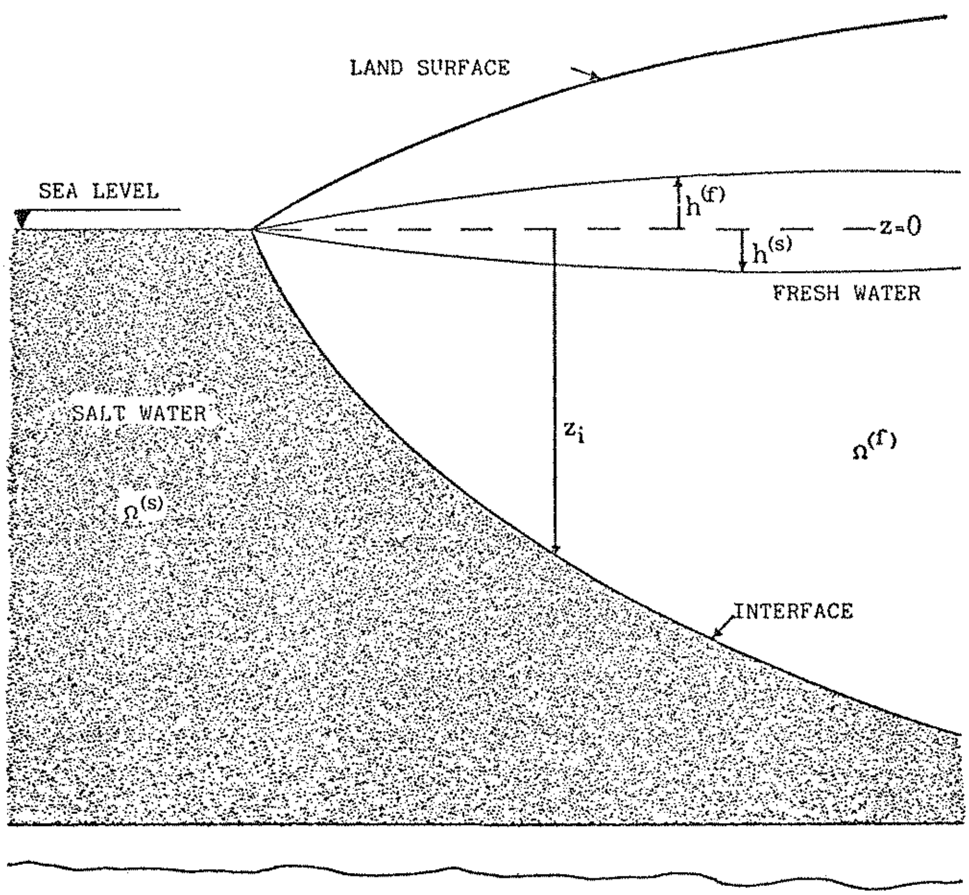

Fig. 2 - Pinder's geometric schematization.

to seawater intrusion, i.e. to the peculiar phenomenon due to the permeability of the coastal soil whereby seawater flows into the aquifer. This phenomenon may be schematized in various ways which can be translated into suitable analytical expressions.

In each case, the description of the phenomenon of seawater intrusion is very difficult to treat as it also affects the hydrodynamic conditions of the freshwater lens. In addition to Ghyben-Herzberg's simple hydrostatic relation, (Fig. 1) numerous treatments of the problem have appeared in the literature. The one chosen for our present purposes is that of G.F. Pinder [3].

This treatment is based mainly on the analysis of two filtration flows i.e. those of freshwater and salinewater, the interactions between which are described by a suitable equation of pressure equilibrium at the interface. With reference to the geometric schematization shown in Fig. 2 and on the basis of simplifying hypotheses similar to those usually put forward to describe filtration motions, the phenomenon is represented by the pair of equations:

$$\frac{\partial}{\partial x}\left(T^{(f)}\frac{\partial h^{(f)}}{\partial x}\right)+\frac{\partial}{\partial y}\left(T^{(f)}\frac{\partial h^{(f)}}{\partial y}\right)=Q^{(f)}+\left(\varepsilon_o+\varepsilon_1\,\rho_*^{(f)}+S^{(f)}\right)\frac{\partial h^{(f)}}{\partial t}-$$

$$-\varepsilon_1\,\rho_*^{(s)}\frac{\partial h^{(s)}}{\partial t}\quad \text{inside}\ \left\{\Omega^{(f)}\right\} \tag{1}$$

$$\frac{\partial}{\partial x}\left(T^{(s)}\frac{\partial h^{(s)}}{\partial x}\right)+\frac{\partial}{\partial y}\left(T^{(s)}\frac{\partial h^{(s)}}{\partial y}\right)=Q^{(s)}+\left(\varepsilon_1\,\rho_*^{(s)}+S^{(s)}\right)\frac{\partial h^{(s)}}{\partial t}-$$

$$-\varepsilon_1\,\rho_*^{(f)}\frac{\partial h^{(f)}}{\partial t}\quad \text{inside}\ \left\{\Omega^{(s)}\right\}$$

where H = hydraulic head
T = transmissivity
S = storage coefficient
Q = specific flow injected or extracted
ε_i = actual porosity in the vicinity of the interface
ε_o = actual porosity in the vicinity of the free surface.

$$\rho_*^{(f)}=\rho^{(f)}\,/\,(\rho^{(s)}-\rho^{(f)})$$

$$\rho_*^{(s)}=\rho^{(s)}\,/\,(\rho^{(s)}-\rho^{(f)})$$

$\rho^{(f)}$, $\rho^{(s)}$ = freshwater and salinewater density.

The superscripts (f) and (s) indicate that the quantities refer to the freshwater zone, and the seawater zone, respectively.

In order to calculate the distribution of the piezometric $h^{(f)}$ and $h^{(s)}$ at a given time t, the boundary conditions must of course be added to equations (1) as follows:

$$\begin{aligned} h^{(f)}(x,y,t) &= \bar{h}^{(f)}(x,y,t) \\ h^{(s)}(x,y,t) &= \bar{h}^{(s)}(x,y,t) \end{aligned} \qquad (2)$$

on $\sum$, boundary between $\Omega^{(f)}$ and $\Omega^{(s)}$

as well as the initial conditions:

$$\begin{aligned} h^{(f)}(x,y,o) &= h_o^{(f)}(x,y) \quad \text{inside} \quad \Omega^{(f)} \\ h^{(s)}(x,y,o) &= h_o^{(s)}(x,y) \quad \text{inside} \quad \Omega^{(s)} \end{aligned} \qquad (3)$$

where $\bar{h}^{(f)}$, $\bar{h}^{(s)}$, $h_o^{(f)}$ and $h_o^{(s)}$ are to be considered as known values.

Lastly, the interface pressure is given by the expression:

$$z_i = \frac{h^{(s)}\rho^{(s)} - h^{(f)}\rho^{(f)}}{\rho^{(s)} - \rho^{(f)}} \qquad (4)$$

The use of G.F. Pinder's model with its rather complex analytical developments is decided on the basis of the availability of the data of the various parameters it refers to.

However, a few considerations may be made for the sake of simplicity. Firstly, unless peculiar conditions occur, it is easy to ascertain that the effect of the storage coefficients $S^{(f)}$ and $S^{(s)}$ is quite negligible, so that it is not strictly necessary to know them.

On the other hand, the trasmissivities $T^{(f)}$ and $T^{(s)}$ may be derived from a knowledge of the aquifer's permeability and from an estimation of the position of the free surface and the interface.

Lastly, as an approximation, it is possible to give zero values to the boundary and initial conditions $\bar{h}^{(s)}$ and $h_o^{(s)}$ on the hypothesis that the seawater is motionless in the presence of freshwater stationary motion.

The approximations thus introduced mostly lead to errors of the same order of magnitude as those due to the application of linear equations to an unconfined aquifer.

3. APPLICATIONS

Within the framework of applications of global methodologies of groundwater management, an aquifer has been chosen on the Ionian coast of Puglia, extending from Gallipoli in the direction of Taranto (Fig. 3). This groundwater system has an area of some 600 Km^2 and floats on saline water intrusions.

It tends to become thinner as it approaches the coastline, disappearing completely on reaching it, at a point where the permeability of the outcropping rocks allows the flow of the groundwater towards the sea.

On the basis of considerable amount of field studies [2] carried out, an underground watershed may be said to exist upstream from the area in question, which separates the groundwater flowing towards the Ionian Sea from that flowing towards the Adriatic Sea and which, in this area, coincides with the isophreatic countour 2.5 m a.s.l. To the North-West the aquifer borders on the Murge hydrogeological system after rather rapid variations in a number of significant characteristics such as piezometric head, seepage velocity, etc... The neighbouring area to the South-West, on the other hand, does not drain groundwater from the area under examination, and indeed is a tributary to it. Both these boundaries may be considered as coinciding with the same isophreatic line 2.5 m a.s.l. The aquifer under examination may thus be said to be bounded, as well as by the sea, by the isophreatic contour 2.5 m a.s.l.; along its entire perimeter, although with varying conditions of flow exchange with the surrounding aquifers.

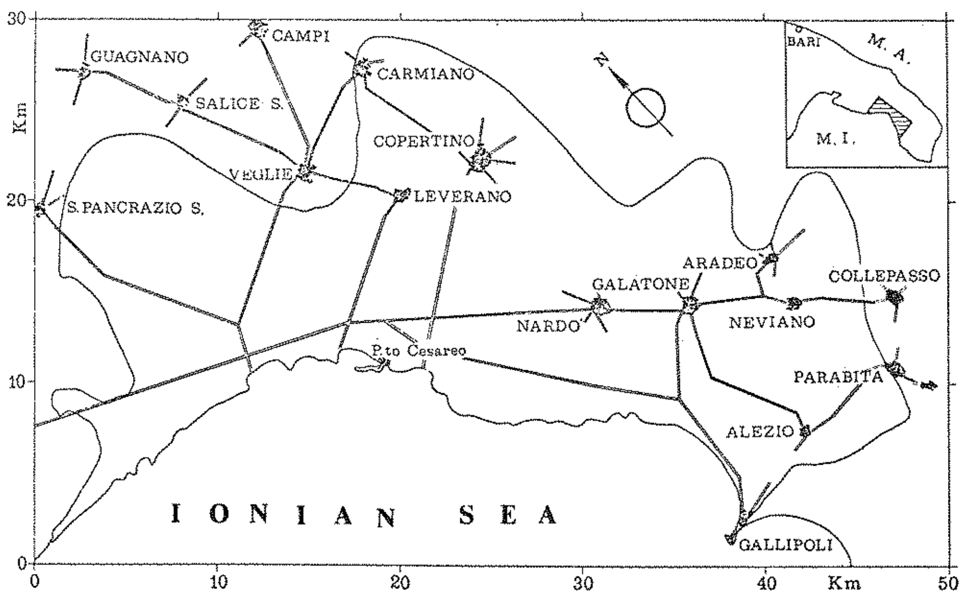

Fig. 3 – Nardò aquifer and the towns in it.

Before G.F. Pinter's model could be applied to it, the aquifer had to be discretized into a network comprising about 1.000 grids, each representing a square-shaped area with a side lenght of 800 m.

The equations of the model then integrated numerically using the finite difference method [5].

$$-\frac{1}{2}T^{(f)}_{i,j+1/2}h^{(f)}_{i,j+1,k+1}-\frac{1}{2}T^{(f)}_{i-1/2,j}h^{(f)}_{i-1,j,k+1}+$$
$$\left[\frac{(\Delta x)^2}{\Delta t_{k+1/2}}(\varepsilon_{i,j}+\varepsilon_{i,j}\rho^{(f)}_{*}+S^{(f)}_{i,j})+\frac{1}{2}(T^{(f)}_{i+1/2,j}+T^{(f)}_{i-1/2,j}+\right.$$
$$\left.T^{(f)}_{i,j+1/2}+T^{(f)}_{i,j-1/2})\right]h^{(f)}_{i,j,k+1}-\frac{1}{2}T^{(f)}_{i+1/2,j}h^{(f)}_{i+1,j,k+1}-$$
$$\frac{1}{2}T^{(f)}_{i,j-1/2}h^{(f)}_{i,j-1,k+1}-\frac{(\Delta x)^2}{\Delta t_{k+1/2}}\varepsilon_{i,j}\rho^{(s)}_{*}h^{(s)}_{i,j,k+1}=$$
$$\frac{1}{2}T^{(f)}_{i+1/2,j}h^{(f)}_{i+1,j,k}+\frac{1}{2}T^{(f)}_{i-1/2,j}h^{(f)}_{i-1,j,k}+\frac{1}{2}T^{(f)}_{i,j+1/2}h^{(f)}_{i,j+1,k}+$$
$$\frac{1}{2}T^{(f)}_{i,j-1/2}h^{(f)}_{i,j-1,k}+\left[\frac{(\Delta x)^2}{\Delta t_{k+1/2}}(\varepsilon_{i,j}+\varepsilon_{i,j}\rho^{(f)}_{*}+S^{(f)}_{i,j})-\right.$$
$$\left.\frac{1}{2}(T^{(f)}_{i+1/2,j}+T^{(f)}_{i-1/2,j}+T^{(f)}_{i,j+1/2}+T^{(f)}_{i,j-1/2})\right]h^{(f)}_{i,j,k}-$$
$$\frac{(\Delta x)^2}{\Delta t_{k+1/2}}\varepsilon_{i,j}\rho^{(s)}_{*}h^{(s)}_{i,j,k}-Q^{(f)}_{i,j,k+1/2};$$

$$-\frac{1}{2}T^{(s)}_{i,j+1/2}h^{(s)}_{i,j+1,k+1}-\frac{1}{2}T^{(s)}_{i-1/2,j}h^{(s)}_{i-1,j,k+1}+$$
$$\left[\frac{(\Delta x)^2}{\Delta t_{k+1/2}}(\varepsilon_{i,j}\rho^{(s)}_{*}+S^{(s)}_{i,j})+\frac{1}{2}(T^{(s)}_{i+1/2,j}+T^{(s)}_{i-1/2,j}+\right.$$
$$\left.T^{(s)}_{i,j+1/2}+T^{(s)}_{i,j-1/2})\right]h^{(s)}_{i,j,k+1}-\frac{1}{2}T^{(s)}_{i+1/2,j}h^{(s)}_{i+1,j,k+1}-$$
$$\frac{1}{2}T^{(s)}_{i,j-1/2}h^{(s)}_{i,j-1,k+1}-\frac{(\Delta x)^2}{\Delta t_{k+1/2}}\varepsilon_{i,j}\rho^{(f)}_{*}h^{(f)}_{i,j,k+1}=$$
$$\frac{1}{2}T^{(s)}_{i+1/2,j}h^{(s)}_{i+1,j,k}+\frac{1}{2}T^{(s)}_{i-1/2,j}h^{(s)}_{i-1,j,k}+$$
$$\frac{1}{2}T^{(s)}_{i,j+1/2}h^{(s)}_{i,j+1,k}+\frac{1}{2}T^{(s)}_{i,j-1/2}h^{(s)}_{i,j-1,k}+\left[\frac{(\Delta x)^2}{\Delta t_{k+1/2}}(\varepsilon_{i,j}\rho^{(s)}_{*}+S^{(s)}_{i,j})-\right.$$
$$\left.\frac{1}{2}(T^{(s)}_{i+1/2,j}+T^{(s)}_{i-1/2,j}+T^{(s)}_{i,j+1/2}+T^{(s)}_{i,j-1/2})\right]h^{(s)}_{i,j,k}-$$
$$\frac{(\Delta x)^2}{\Delta t_{k+1/2}}\varepsilon_{i,j}\rho^{(f)}_{*}h^{(f)}_{i,j,k}-Q^{(s)}_{i,j,k+1/2};$$

Several tests were carried out in this aquifer: two of these are discussed in the following. In the first only 1 pumping well was used for drawing out freshwater, in the second 25 distribute in the whole aquifer area (Fig. 4).

These schematizations are sufficiently representative to allow an understanding of the behaviour of the aquifer. It was hypothesized, starting from totally undisturbed conditions. In first test a pumping well was set up in the aquifer to extract freshwater at a given constant flowrate. The analysis carried out refers to behaviour of the perturbation set up by this extraction both in the freshwater zone and the saline water zone which, by means of the expression (4), enabled also the variations in the position of the interface to be evaluated.

Fig. 5 shows the diagrams of the variations with respect to time of the freshwater head $\Delta H_p^{(f)}$ and of the saline water head $\Delta H_p^{(s)}$ at the pumping well. Of particular interest is the comparison with the result obtained from a model that neglects saline water motion (curve $\Delta h^{(f)}$).

The most significant of the various observations that could be made in this connection is how G.F. Pinder's model predicts a non-steady condition which is much more prolonged in time. Infact, a fortnight after pumping began the variation induced in the freshwater head attained only 45% of the final value according to the G.F. Pinder's model, and as much as 85% of the final value according to the model neglecting saline water motion.

The inertia, Pinder's model shown, could be attributed to the major water volume, which was necessary to draw out in order to attaining the equilibrium configuration.

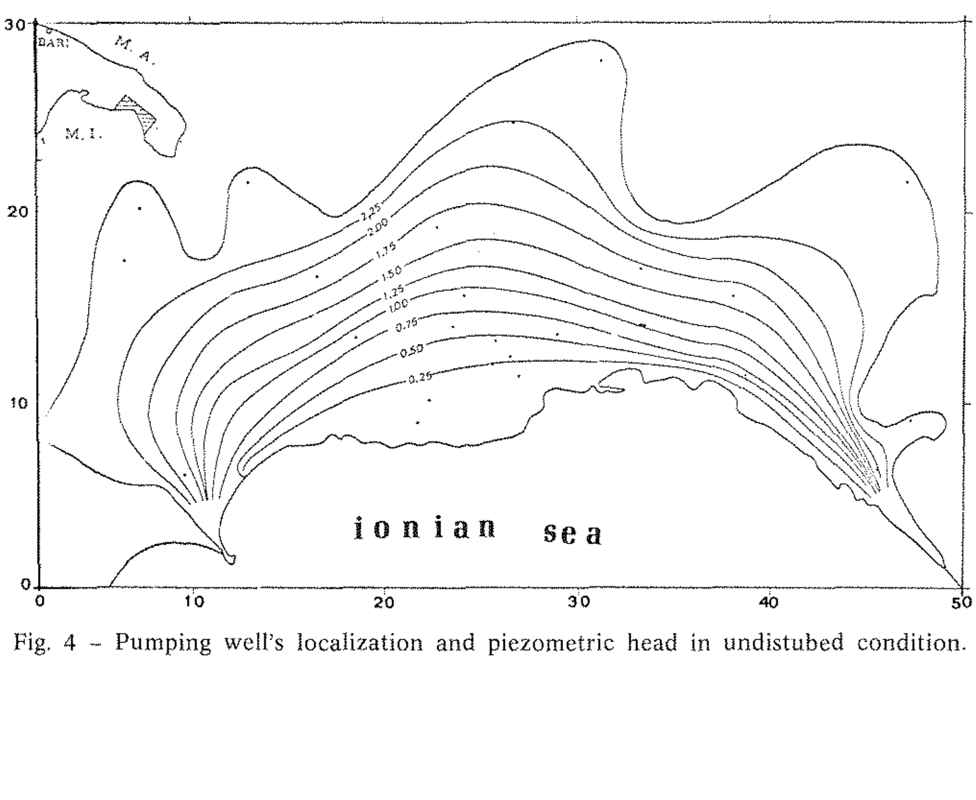

Fig. 4 – Pumping well's localization and piezometric head in undistubed condition.

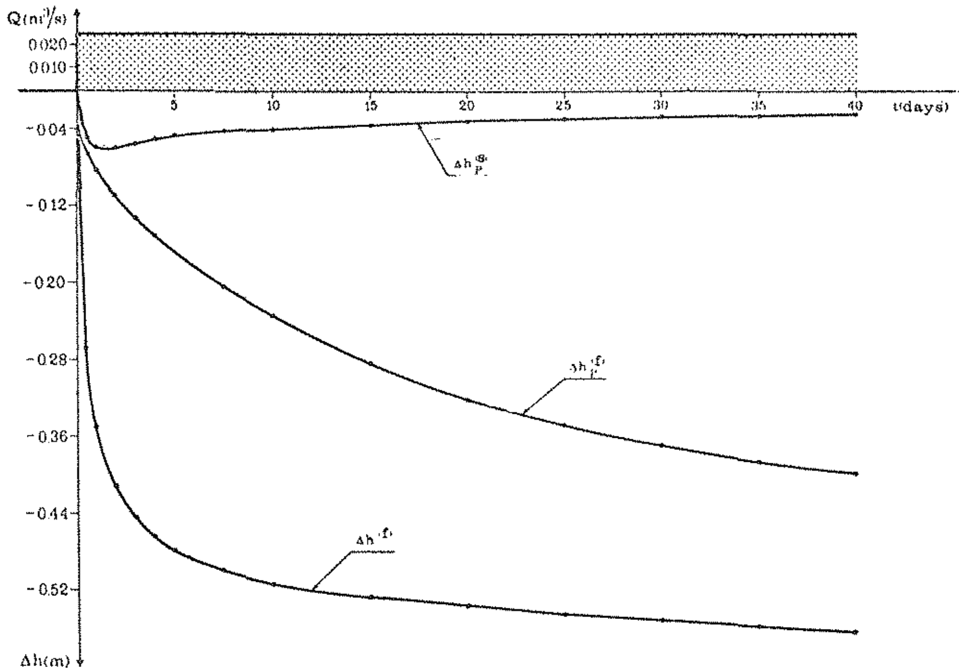

Fig. 5 – The comparison between freshwater and salt water in Pinder's model neglecting saline water motion for 1 pumping well.

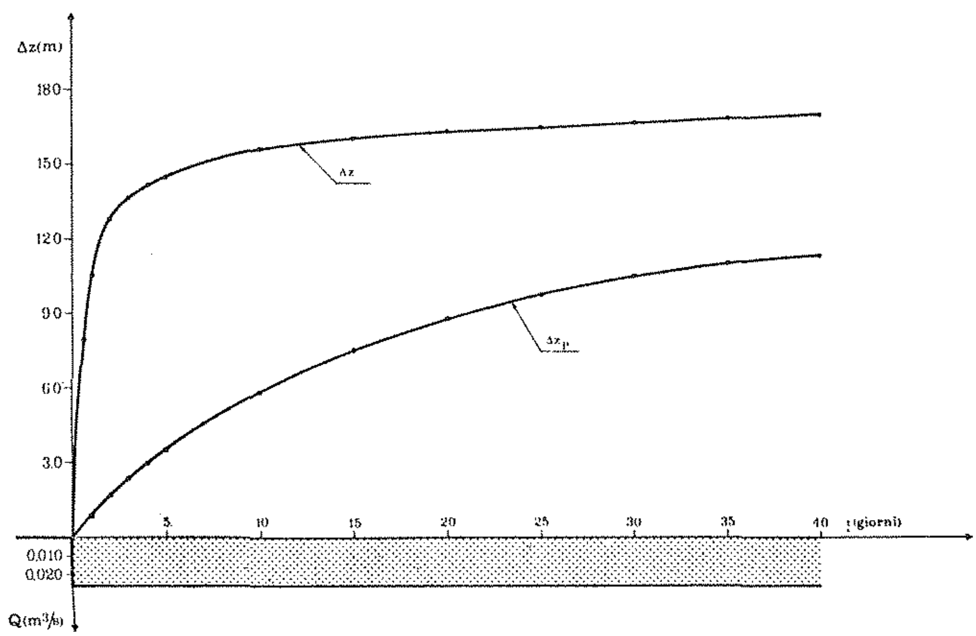

Fig. 6 – The variation of interface of Pinder's balance equation and Ghyben-Herzberg's equation for 1 pumping well.

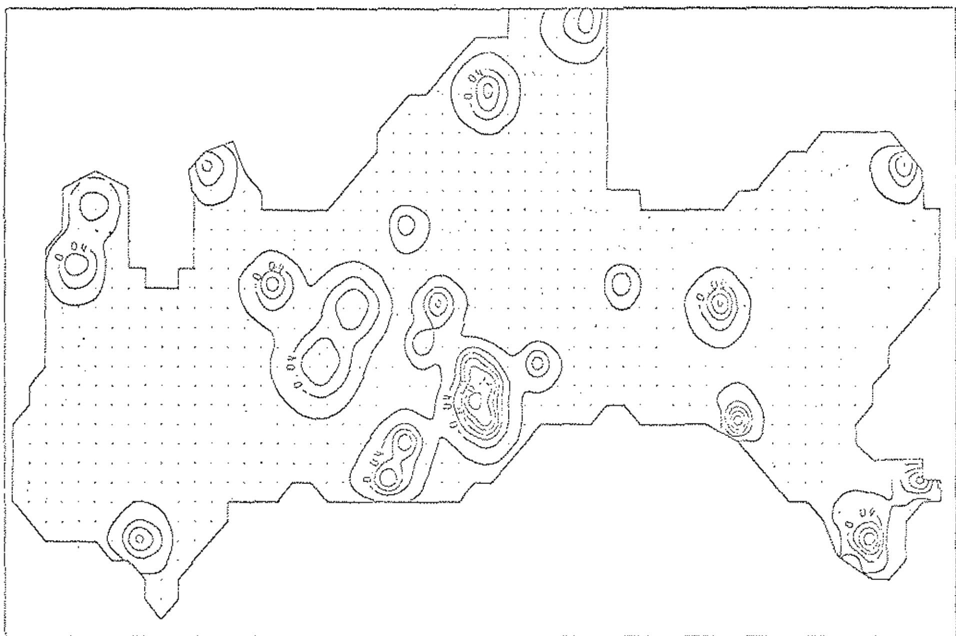

Fig. 7 - The drawdown of the salt water head with Pinder's model.

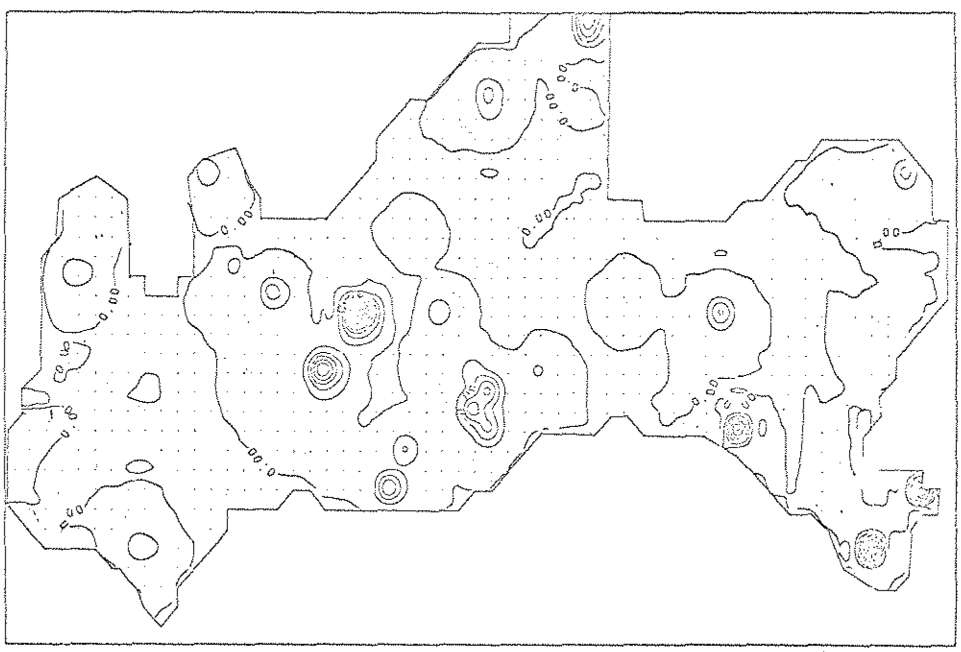

Fig. 8 - The drawdown of the freshwater head with Pinder's model.

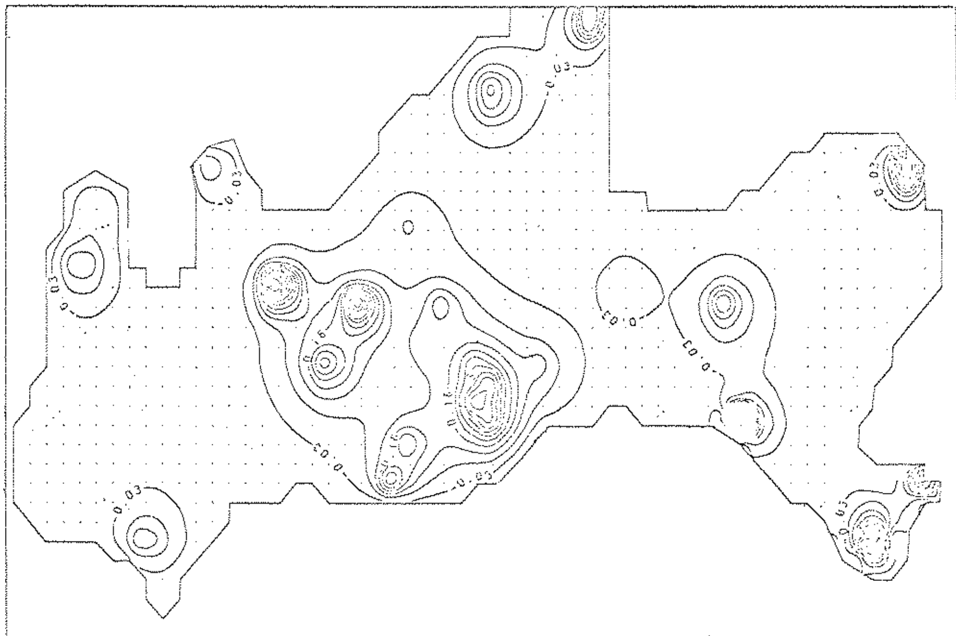

Fig. 9 – The drawdown of the freshwater head with the model that neglects saline water motion.

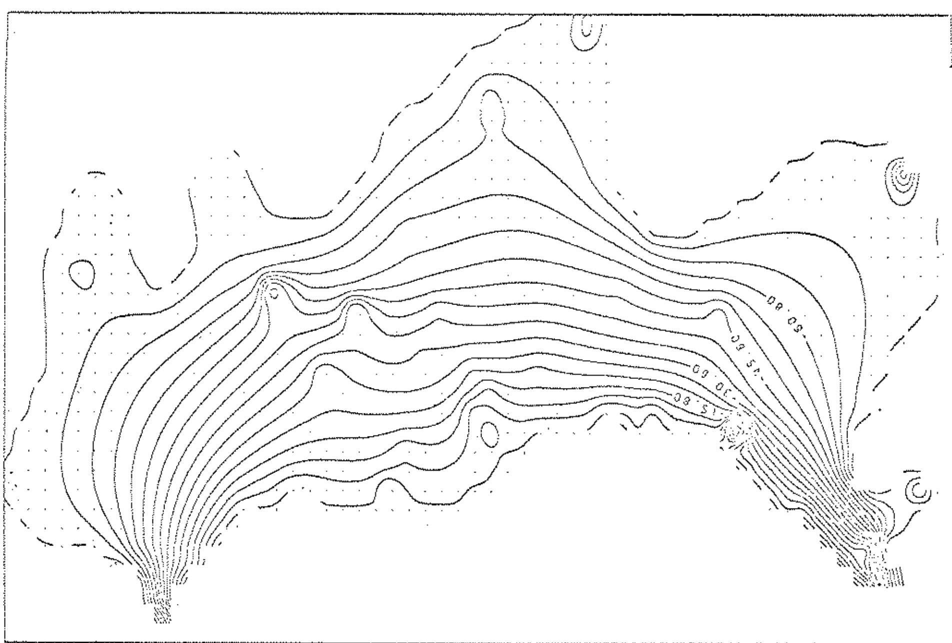

Fig. 10 – The interface calculated with Ghiben-Herberg's scheme.

In such views, the contamination of a coastal aquifer takes along time before its full accomplishment, which is characterized by having brackish water in the pumping well. This must be kept into consideration drawing water from a newly drilled facility, because saline water can appear much later than expected by means of empiric forecasts.

The greater inertia of a fully movable aquifer is probably also the cause of the well known stability of the groundwater contamination, after being accomplished, which persisting for extremely long time, is practically considered as irreversible.

Fig. 6 shows the changes in the position of the freshwater and saline water interface according to the G.F. Pinder's model, Δz_p again compared with the model prediction for saline water with evaluation of the interface position according to Ghyben-Herzberg's scheme, Δz.

These comparisons showed that G.F. Pinder's model, which provides a more detailed description of the interaction between freshwater and saline water allows useful indications to be obtained concerned possible pumping under equivalent conditions of risk of pollution by sea water.

In the second test 25 pumping wells were operated to draw out freshwater at a given constant flowrate (25 l/s), in order to evaluate the model behaviour and then the interactions amoung the pumping wells, how was shown in Fig. 7.

For the variations of the freswater head, this test allowed to confirm the considerations drawn in the other one, when Pinder's model (Fig. 8) and the model that neglects saline water motion (Fig. 9) were compared.

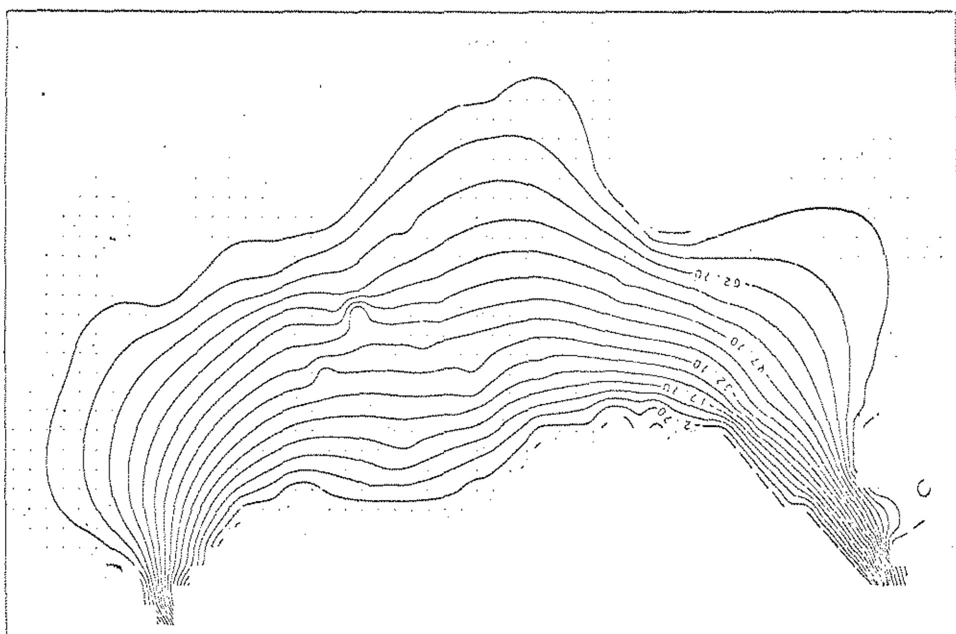

Fig. 11 - The interface calculated with Pinder's model.

The comparison of the two models with regard to the modeling of the interface (Fig. 10-11) allowed us to conclude that the approximation of Pinder's model puts in evidence the big inertia of the system: the water drawing up then less dangerous and, therefore, the resource could be utilized with less risk.

Obviously, in order to obtain the critic pumping flowrate it would be necessary to apply Pinder's model to the diffusion zone.

ACKNOWLEDGEMENTS

Thanks are due to Mr. Soria for technical and computering assistance.

REFERENCES

1 - BARAGLIA R., SORIA B.: *Installazione sotware Calcomp GPCP-II e THREED.* Rapporto CNUCE 190. 1982.

2 - COTECCHIA V.: *Studi e Ricerche sulle acque sotterranee e sulla intrusione marina in Puglia (Penisola Salentina).* Quaderno IRSA-CNR n. 20 (1973).

3 - PINDER G.F.: *A Galerkin Finite Element Simulation of Ground-Water contamination on Long-Island, New York.* Water Resources 9, (6), 1657, 1973.

4 - SIRANGELO B., TROISI S.: *Studio Metodologico di nuove tecniche di Gestione di Risorse Idriche Sotterranee.* 1. Modello di Simulazione Idrodinamica Idrosim. Quaderno IRSA-CNR n. 50, 1980.

5 - SMITH G.D.: *Numerical Solution of Partial Differential Equation: Finite difference methods.* Clarendon Press, Oxford, 1978.